Can full waveform refraction imaging overcome the century-long impasse at the first breaks?

Derecke Palmer
The University of New South Wales
Sydney 2052 Australia
d.palmer@unsw.edu.au

SUMMARY

The signal-to-noise ratios (SNR) of the first arrivals are a function of the source-to-receiver distance and the head wave coefficient (HWC), the refraction analogue of the reflection coefficient. In turn, the precision of the first break traveltimes is a function of the SNR.

Stacking with the refraction convolution section (RCS) can significantly reduce the effects of geometrical spreading. However, the effects of the HWC still remain.

The time models of the base of the weathering computed with the common reciprocal method are comparable to those computed with the RCS. However, only the RCS is able to detect small thrusts within the Fresnel zone.

Key words: first breaks, precision, signal-to-noise, RCS.

THE IMPASSE AT THE FIRST BREAKS

In the last 50 years, exploration reflection seismology has undergone many far-reaching advances. They include common midpoint (CMP) stacking, signal processing, 3D methods, pre-stack time and depth migration, attribute analysis, and full waveform inversion (FWI). These advances have been driven by the ongoing objectives of all methods of seismic exploration which are to improve resolution and signal-to-noise ratios (SNR) (Brown, 2011, Figure 1.3). As a result, there are very few areas where current seismic reflection technology fails to generate useful results.

By contrast, refraction seismology has yet to realize any comparable advances. The vast majority of seismic refraction methods, whether they be employed for statics corrections, geotechnical or crustal investigations, still only employ scalar traveltimes. There are no widely accepted methods for acquiring, processing and presenting seismic refraction data which are comparable to the full waveform images routinely generated with seismic reflection data (Cox, 1999, p.218). Accordingly, the majority of present-day implementations of refraction seismology can be viewed as representative of a 50 year old technology, refraction tomography notwithstanding.

It can be speculated that a major reason for the longstanding failure to adopt simple methods of full waveform refraction imaging and processing, has been the traditional paradigm that precise travelimes are both essential and more useful than the analysis of full waveform images. As a result, routine near surface seismic refraction investigations have been stalled at the first breaks for almost a century.

ARE PRECISE TRAVELTIMES ESSENTIAL?

Any search of the literature will reveal numerous studies which describe disparate methods for picking first arrival traveltimes (Khalaf et al, 2018). In most near surface refraction investigations, the objective is to measure traveltimes to a precision of better than a millisecond, independently of the SNRs. It is often claimed that precise traveltimes are an essential prerequisite for producing high resolution refraction tomograms.

Nonetheless, Palmer (2015a), demonstrates that the RMS misfits with refraction tomography are approximately 5 milliseconds for a range of 1D, 1.5D and 2D starting models, whereas the precision of the traveltime data is better than 1 millisecond. It can be concluded that the resolution of any refraction tomogram is related more to the accuracy of the starting model, than to the precision of the traveltime data.

Given the smoothing inherent in tomographic inversion (Palmer, 2015a), are precise first break traveltimes essential?

OBJECTIVES

The major objective of this study is to demonstrate that full waveform refraction imaging and processing with the refraction convolution section (RCS) (Palmer, 2001) can usefully employ the same operations of CMP stacking and signal processing as are standard practice with exploration reflection seismology. These operations address three fundamental issues which are related to SNRs and resolution.

First, the geometric spreading component of the head wave amplitude varies as approximately as the inverse square of the source-to-receiver distance. In this study, it exhibits an extremely large range of more than 80 dB. Since the first break traveltimes are measured where the SNR is a minimum, it is inevitable that the precision of any first break traveltimes will vary with the source-to-receiver distance.

Second, the head wave amplitude is also a function of the head wave coefficient (HWC), which is the refraction analogue of the reflection coefficient. In this study, the HWC varies by a factor of approximately 4 or 12 dB.

Third, full waveform images enable the routine application of deconvolution, which usually results in major improvements in vertical resolution. It facilitates the detection of detailed geological structures within the refraction Fresnel zone.

THE DATA

This study employs the data for a 2 km section of the Wirrinya traverse 99WR-HR1, which was recorded over 17 km of the Palaeozoic Lachlan Fold Belt in south-eastern Australia. The data were recorded with 240-channel split spreads and bunched receivers 10 metres apart with two adjacent 30 tonne vibrators generating two 5 second 12-140 Hz sweeps (Jones and Drummond, 2001). The source interval is generally 20 m.

This section has been selected because detailed models of the P-wave seismic velocities in the sub-weathered region have been computed previously from the traveltime data with 1.5D and 2D inversion algorithms (Palmer, 2015a). The various refraction tomograms, which exhibit considerable spatial variations in the seismic velocities in the sub-weathered region, are representative of a moderately complex geological environment. Furthermore, a lateral change in the seismic velocities in the weathered layer, which occurs between stations 1465 and 1500, has a significant effect on the HWC.

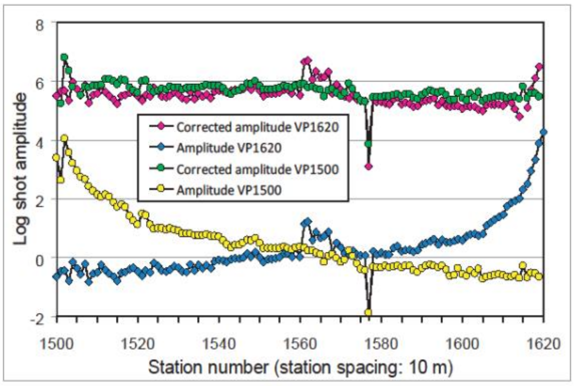

Figure 1: Measured and offset corrected shot amplitudes

Figure 1 presents the measured head wave amplitudes for two reversed shot records, together with the values corrected for the geometric spreading. Figure 1 shows that the head wave amplitudes of the Wirrinya data vary by more than four orders of magnitude (0.3 – >3000), that is, by more than 80 dB ($20\, log(3000/_{0.3})$) By contrast, the offset corrected head wave amplitudes vary by less than one order of magnitude.

MEASURING TRAVELTIMES ON COG

In this study, the traveltimes and amplitudes were measured on common offset gathers (COG). Whereas the amplitudes and traveltimes are usually measured on common shot gathers, there can be major operational conveniences with reformatting the data into COG gathers, largely because the variations in the traveltimes and the SNRs between adjacent traces are greatly reduced. The reformatting from the shot record domain into the COG domain enables the use of horizon picking software routinely employed with seismic reflection processing and interpretation.

The use of automatic horizon picking software on COG gathers can avoid many of the ambiguities associated with the various criteria for defining the first break, all of which are affected in varying degrees by the SNRs. It can enable a more objective measure of the traveltime.

Furthermore, the amplitudes and traveltimes are measured where the SNRs are a maximum at the centre of the wavelet which is a trough, and which is appropriate for the zero phase data used in this study. It can be reasoned that the traveltimes are more precise and more consistent than those picked at the first detectable arrival of energy, that is, at the first break, where the SNRs are a minimum.

2D CRM MULTI-FOLD TIME MODELS

The common reciprocal method (CRM) algorithm for the computation of a 2D time model explicitly identifies forward and reverse traveltimes, and therefore, it can accommodate dipping and/or irregular interfaces. However, there can be bulk or “static” shifts between overlapping sets of computations with multi-fold data, because of errors in the reciprocal times. Therefore, rather than relying on the precision of a single measurement of the reciprocal time from the shot records, a two stage process, which computes an average reciprocal time over a multiplicity of receiver locations, is employed (Palmer, 2009).

First, so-called “long wavelength” time models are generated at each source location with forward and reverse intercept times. For each shot pair in each direction of recording, a single time model is computed from a multiplicity of reciprocal times. For a cross-over distance of 20 stations, up to 80 reciprocal times are employed (120 traces minus 20 station source separation minus 20 station cross-over distance (Palmer 2015a, Figure 4)). The forward and reverse intercept time models at each location are then averaged to generate a single long wavelength time model at each source location.

Second, so-called “short wavelength” time models are generated at each receiver location using the CRM algorithm. The CRM algorithm generates time models at a multiplicity of receivers with a single reciprocal time for each pair of forward and reverse shot records.

In the CRM computations in this study, the separation between the forward and reverse sources is 120 stations. However, the first 20 values in each direction of recording are disregarded, corresponding with the cross-over distance. Therefore, 80 time models are computed for each shot pair. However, the source spacing is generally two stations. Therefore, there are only 40 coincident long and short wavelength parameters.

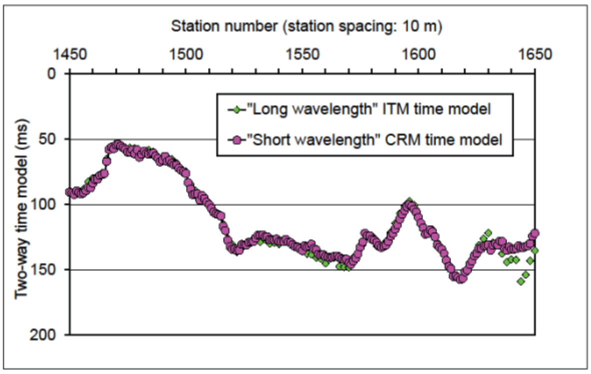

Figure 2: Multi-fold long wavelength ITM and short wavelength CRM time models.

The reciprocal time for each shot pair is recovered by averaging the differences between the 40 coincident long and short wavelength time models at common locations. The resulting reciprocal times, which generally have a precision of the order of a millisecond, are also employed in the generation of the stacked refraction convolution section (RCS).

Up to 40 short wavelength time models are generated at each receiver location, and accordingly, an average is taken. Figure 2 presents the multi-fold long and short wavelength CRM time models.

THE STACKED RCS

The essential process for the generation of the short wavelength time model with the CRM is the addition of the forward and reverse scalar traveltimes. The RCS achieves the equivalent process through the convolution of the corresponding seismic traces, since convolution adds phase, that is, traveltimes, and multiplies amplitudes (Palmer, 2001). Therefore, the stacked RCS corresponds with the averaged short wavelength time model. The stacked RCS constitutes an arithmetic, rather than a geometric average of the amplitude products.

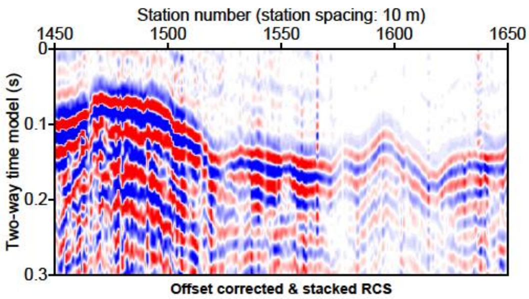

Figure 3: The stacked RCS, generated with shot records corrected for geometric spreading.

Figure 3 presents the stacked RCS. It is generated by (i) correcting each trace for geometric spreading, (ii) convolving pairs of corrected shot records for which the source separation is 120 stations, (iii) subtracting the reciprocal time for each convolved shot pair, (iv) a CMP sort and gather and finally, (v) diversity stacking. Fold is generally 40. The amplitudes of the stacked RCS are measured prior to further processing, such as deconvolution and trace balancing.

The HWC shown in Figure 4 are the square root of the measured RCS amplitudes, because convolution multiplies the shot amplitudes. The range of amplitudes in Figure 3 is 24 dB ($2 * 20\, log\left({}^{160}/_{40}\right)$), which is considerably less than the 80 dB of the shot records.

STACKING WITH NO OFFSET CORRECTION

A useful result of convolution is that, to a good first approximation, the multiplication of the amplitudes significantly reduces the considerable variation in amplitude with offset with refraction data (Palmer, 2001, Figure 8). Figure 4 presents a comparison of the head wave coefficients derived from the stacked RCS which has had a correction for geometric spreading applied before convolution, and the stacked RCS to which no corrections have been applied. The correlation coefficient is 0.968.

It can be concluded that convolution and stacking with multi-fold data has effectively compensated for the extremely large geometric spreading of the shot records. Furthermore, the generally 40 fold stack represents an averaging of the residual geometric effect over a distance of 800 m.

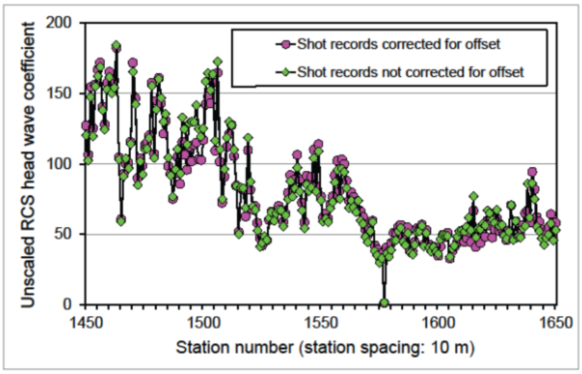

Figure 4: Comparison of the head wave coefficients derived from the stacked RCS which has had a correction of geometric spreading applied before convolution, and the stacked RCS to which no corrections have been applied.

COMPARISON OF CRM & RCS TIME MODELS

Figure 5 presents the stacked and trace balanced, but not deconvolved RCS and the CRM time model. It demonstrates excellent agreement with both the short and long wavelength variations. While most of the long wavelength variations in the time model can be recognized in the 1.5D and 2D refraction tomograms in Palmer (2015a), the short wavelength variations, which can be attributed to the very near surface soil layers, have been removed with tomographic inversion.

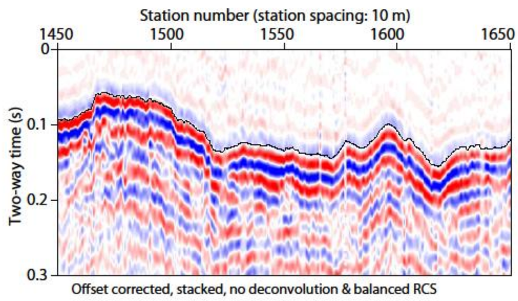

Figure 5: The stacked RCS without deconvolution and the CRM time model.

The RCS has substantially better SNR than a single trace, due to the approximate 40 fold (20 log√40=16 dB). Nevertheless, the multi-fold CRM derived time model is several milliseconds earlier than the RCS first arrivals between approximately stations 1525 and 1650. In that region, the head wave amplitudes, as indicated with the HWCs in Figure 4, are lower than elsewhere. It demonstrates that the precision of the first break traveltimes is related to SNRs. It also provides a measure of the relative difference between picking traveltimes at the first break, versus at the first extremum. In view of the close agreement between the CRM time model and RCS first arrivals, this study questions whether the measurement of precise first arrival traveltimes *on the shot records* is an essential prerequisite for the computation of a detailed time model of the base of the weathering.

RESOLUTION WITHIN THE FRESNEL ZONE

Nevertheless, it can be reasoned that the major issue is not whether the traveltime is measured at the first break or the first extremum, but rather the fact that only a single scalar value is obtained. With the greater vertical resolution which follows with the application of deconvolution, Figure 6 demonstrates that a probable small thrust fault occurs at station 1496. Although the CRM is able to resolve comparable changes in the time model at stations 1480 and 1506, it generates a smoothed or averaged time model at station 1496.

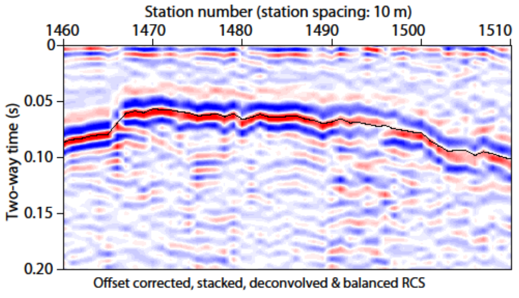

Figure 6: The deconvolved RCS indicates small scale thrust faults which are not apparent in the CRM time model.

Whereas the CRM computes the time model with the addition of the forward and reverse scalar traveltimes, the RCS achieves the same mathematical result, through the convolution of the complete forward and reverse traces, *prior* to the measurement of any scalar traveltimes. Therefore, the RCS reverses the traditional procedure of the measurement of traveltimes followed by the processing of the data. As a result, the seismic wavelet is preserved through to the next stage of the processing routine, and the detailed resolution of any structure within the refraction Fresnel zone is enabled with the stacked RCS. Further significant improvements in structural resolution are achieved with deconvolution.

The superior structural definition of the full waveform imaging of the RCS, when compared with the scalar traveltime model, is demonstrated with an even more complex geological structure at station 1467. The RCS is still able to generate a useful image of the base of the weathering, because it indicates the occurrence of the shallowly dipping refracting interface within the Fresnel zone of the refractor, which in this study, represents an important structural feature, namely, another thrust fault.

Palmer (2013, 2015b) demonstrates that even where detailed seismic velocities are employed as starting models, refraction tomography is not able to resolve the dip of any interfaces within the Fresnel zone at the base of the weathering. It is an inevitable result of the ill-posedness of most traveltime-based inversion methods. In turn, it demonstrates the necessity for employing full waveform imaging and/or inversion in order to resolve detailed geological structure.

Therefore, while every effort should be made to derive precise first break traveltimes, primarily to compute precise seismic velocities (Palmer, 2015a), they are unable to resolve accurately even simple structure within the refraction Fresnel zone at the base of the weathering (Palmer, 2013; Palmer, 2015b). Where detailed structure is an important objective, such as in most near-surface investigations, then some form of full waveform imaging, such as with the RCS, can be required. Notwithstanding, first arrival traveltimes, whether measured at the first breaks or the first extremum, can still generate useful starting models with the major part of any investigation. It can be concluded that precise first arrival traveltimes should not be afforded *undue* importance.

CONCLUSIONS

The signal-to-noise ratios (SNR) of the first arrivals are a function of the source-to-receiver distance and the head wave coefficient (HWC), the refraction analogue of the reflection coefficient. In turn, the precision of the first break traveltimes is a function of the SNR.

Stacking with the refraction convolution section (RCS) can significantly reduce the effects of geometrical spreading. However, the effects of the HWC still remain.

The time models of the base of the weathering computed with the common reciprocal method (CRM) are comparable to those computed with the RCS. However, only the RCS detected detailed geological structure within the Fresnel zone.

REFERENCES

Brown, A. R., 2011, Interpretation of three-dimensional seismic data; SEG Investigations in Geophysics, No. 9, 7th edition, Society of Exploration Geophysicists, Tulsa, 646p.

Cox, M. J. G., 1999, Static corrections for seismic reflection surveys. Society of Exploration Geophysicists, Tulsa.

Jones L.E.A. and Drummond B.J. 2001. Effect of smoothing radius on refraction statics corrections in hard rock terrains. *15th ASEG Conference and Exhibition, Brisba*ne (Extended Abstract).

Khalaf, A., Camerlynck, C., Florsch, N., and Schneider, A., 2018, Development of an adaptive multi-method algorithm for automatic picking of first arrival times: application to near surface seismic data. *Near Surface Geophysics* 16, 507-526.

Palmer, D, 2001, Imaging refractors with the convolution section, *Geophysics* 66, 1582-1589.

Palmer D. 2009. Integrating short and long wavelength time and amplitude statics. *First Break* 27(6), 57–65.

Palmer, D., 2013, Resolving complex structure in near-surface refraction seismology with common offset gathers: *The Leading Edge*, 32, 680-690.

Palmer, D., 2015a, Is accuracy more important than precision in near surface refraction seismology? *Near Surface Geophysics*, 13, 1-18.

Palmer, D., 2015b, Does diving wave tomography improve discovery in near surface refraction seismology? *FastTIMES* 20(3) 15-32.